

## Principles of Optimization of Structures Against an Impact

This article has been downloaded from IOPscience. Please scroll down to see the full text article.

2011 J. Phys.: Conf. Ser. 319 012021

(<http://iopscience.iop.org/1742-6596/319/1/012021>)

View [the table of contents for this issue](#), or go to the [journal homepage](#) for more

Download details:

IP Address: 155.101.96.134

The article was downloaded on 21/09/2011 at 21:58

Please note that [terms and conditions apply](#).

# Principles of Optimization of Structures Against an Impact

Andrej Cherkaev\*, Elena Cherkaev†, Seubpong Leelavanichkul‡

September 15, 2011

## Abstract

We describe a macro- and micro-behavior of damageable structures. Damage is understood as a process of irreversible phase transition from an initial to a damaged state. An unstructured material can absorb energy until it melts. However, a tiny portion of this energy yields to a construction's disintegration due to instability of the damage that leads to energy concentration. Appearance of concentrated damage zones, such as cracks or delaminating, destroys the construction. The remains of the disintegrated construction can still absorb large amount of energy. The goal of a rational design is to maximally use the energy absorption ability of a damageable material. We propose a concept of a replaceable protective structure design. Such structure should dissipate maximum energy, be able to spread energy of damage, and the damage process should be as stable as possible. The absorption rate and rate of damage propagation are times amplified by waiting-link structures that we describe below.

## 1 Preliminaries

### 1.1 Protective structures

We investigate a problem of propagation of structural damage, formulate principles of optimization of the impact-protecting structures, and present models of a protective structure with improved characteristics. The designed structures must sustain a sudden impact: they absorb the energy while keep their structural integrity. The goal is in contrast with the conventional optimal design of maximally stiff constructions that are designed to be loaded by a given static load. Commonly used protective devices include car bumpers, helmets, tempered glass, climbing screamers, and woven baskets of hot balloons, see Figure 1.

These very different constructions are all designed to be damaged or destroyed in a collision saving the protected object. These constructions might be used only once, they absorb the collision (impact) energy shielding the protected object and keeping the structural integrity. Both features are equally important. In a collision, a properly designed bumper will be badly damaged, thereby absorbing the energy of impact and saving the vehicle and its passengers. A strong and stiff bumper that stays undamaged while the car is ruined does not fit its purpose. Likewise, an easily damageable bumper does not fit it because it does not absorb enough energy. An optimally designed structure

---

\*Department of Mathematics, University of Utah, Salt Lake City, Utah, USA 84112, [cherk@math.utah.edu](mailto:cherk@math.utah.edu)

†Department of Mathematics, University of Utah, Salt Lake City, Utah, USA 84112, [cherk@math.utah.edu](mailto:cherk@math.utah.edu)

‡Department of Mechanical Engineering, University of Utah, Salt Lake City, Utah, USA 84112, [sleelava@eng.utah.edu](mailto:sleelava@eng.utah.edu)

realizes a familiar recommendation of defensive driving instructions “Choose to hit something that will give way (such as bush or shrubs) rather than something hard”.

The energy density determines the capability of a structure to withstand dynamical loading. In most structures, due to a highly uneven distribution of energy density, localized yielding occurs at a particular location while the total energy associated with fracture may be relatively small. To increase stability, a concept of a bistability has been introduced [1]. In bistable structures, yielding propagates in a larger volume, thus increasing the total fracture energy. A bistable structure may be created by forming a chain or lattice of bistable structural elements [2-4]. Multiple regions of such structure exhibit yielding prior to ultimate failure. Thus, the bistable structures allow for the delocalization of yielding. Based on results of our previous research dealing with the bistable structures and their applications, the present paper formulates optimization principles for constructions and structures designed to sustain a damaging impact.

## 1.2 Elements and features of an impact resistive structure

An amorphous or crystalline material with only micron-range order can absorb energy until it fails locally. The lack of longer-range microstructural order precludes distributing the damage away from a concentrated loading zone. Energy concentration leads to instabilities, such as cracking or delamination, which destroy the structural integrity of a protective structure made from such material. In all unstructured materials, the stress rate decreases with increasing strain due to development of imperfections, opening of micro-cracks, dislocation concentration, amongst other mechanisms. These phenomena lead to stress concentrations that eventually destroy the material sample.

The stress concentration can be reduced by means of bistable structures. A simple bistable structure assembly consists of two roughly parallel brittle-elastic or elastic-plastic components, one of which is longer than the other [1, 2, 3]. When the shorter “sacrificial” element fails (indicated as “first failure” in Fig. 2), the load is assumed by the “waiting element” that was initially inactive. Unlike conventional structures, the bistable structure transforms the energy of an impact into directed traveling waves that dissipate energy throughout a larger domain. Delocalization of damage is achieved by allowing partial internal failure to precede ultimate failure. Due to their morphology, bistable structures become stiffer and stronger when damaged. Such structures would evenly distribute the stress and will be stable even when partially destroyed. Structures with inner instabilities, creating multiple inner breakages that lead to stable structural transformation, transport damage away from impacted zone. As a result, the structure can sustain large deformation

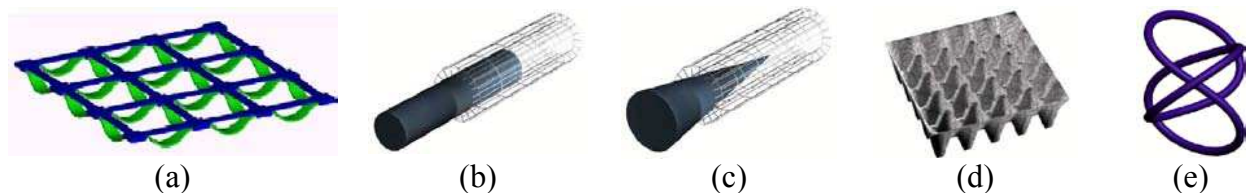


Figure 1: Structures that absorb energy and become partially damaged, but maintain structural integrity. (a) Lattice with redundant load paths. (b) Tube and cylinder. (c) Tube and cone. (d) Multilayer structure. (e) Structure with helices that mimics protein.

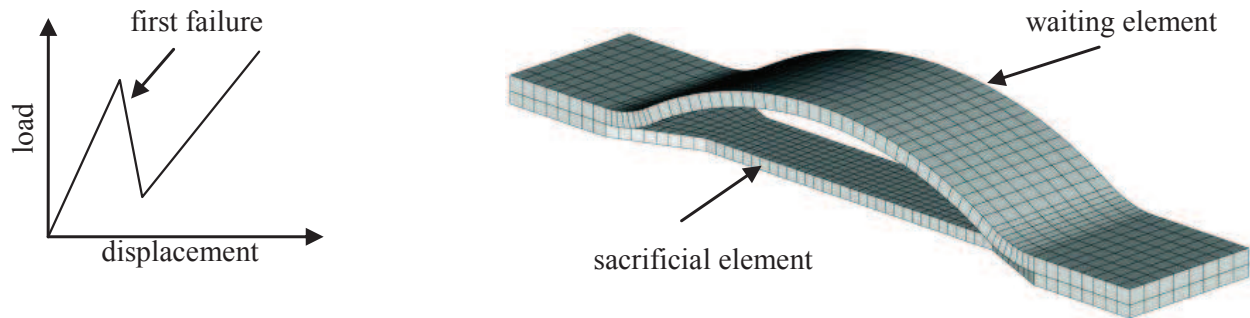


Figure 2: A force-displacement response and a conceptual visualization of a bistable link assembly without total destruction.

### 1.3 Lattices: Stages of structural damage

We study damage of lattice structures that consist of a number of connected rods. A simple frame in Figure 3 illustrates a cascade of breakages. We assume that the rods in the frame are brittle-elastic: the elongation grows with the stress and when it reaches a threshold, the rod fails. Unlike chains with sequentially joined links, lattices are not broken when one or several links fail. We assume that a frame from five breakable rods A, B, C, D, and E is attached to a vertical support and is loaded by a force  $F$  that is applied to the end of rod E, as shown in Figure 3.

The failure of the structure passes through the following stages:

1. Initially, all rods are stressed by a loading  $F$ .
2. When the magnitude of  $F$  increases, rod A breaks. Then, rod B assumes the load; rods C and D become inactive, they form a *waiting link*. The equilibrium remains locally stable but the stiffness of the structure decreases.
3. When rod B fails next, the structure loses its equilibrium and moves to a new equilibrium position that corresponds to straight alignment of rods C and D, which now become active. In the new equilibrium position, the stiffness may increase.
4. Next, one of rods C or D (say, rod C) breaks and the structure moves to another equilibrium position.
5. Finally, rod E breaks and the force is no longer supported by a structure.

Notice, that all rods but D are broken before the load is relieved. The percentage of broken rods shows effectiveness of the support because each breakage absorbs some energy.

Generally, a sequence of breakage of a loaded structure includes: (a) breaks within an equilibrium position, (b) transition from one equilibrium to another one with some waiting links being activated, and (c) a complete breakage when the load is no longer supported by a structure. Step (a) correspond to damage within a stiff structure. An equilibrium of a loaded structure or a sub-structure is called stiff if it corresponds to a local minimum of the energy, that is no node can move without elongating of at least one link and change the energy balance. The number of degrees of

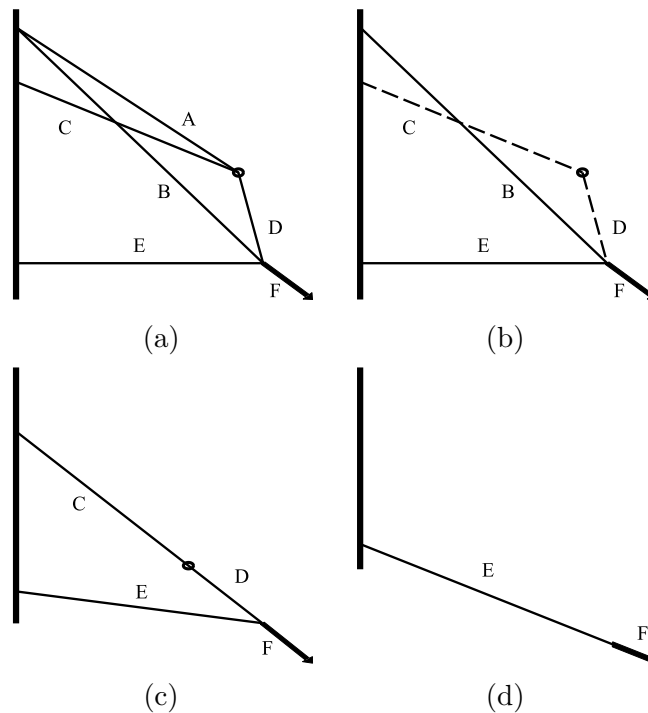


Figure 3: Stages of structural failure

freedom of the nodes of a  $n$ -nodes structure is equal to  $3n$ , out of which 6 degrees correspond to motion of the structure as a solid. The number of active (stressed) links may exceed or be equal to the number of  $3n - 6$  of degrees of freedom of a deformation. In this case, the equilibrium is stiff; moreover, if several active links are removed (broken), the structure remains stiff. When the damaged links are removed, remaining active links redistribute the load, and inactive links are not activated. This process can be analyzed by linearized equilibrium equations. When a certain number of links is removed, the structure loses the stiffness (Step (b)) and moves from the equilibrium point. The motion stops when some previously inactive waiting links are activated and the structure assumes a new equilibrium position. The process repeats, until the structure fails and stops to resist the load. The analysis of this process requires consideration of dynamics since the transitions between equilibria correspond to a significant dynamic load factor that could result in further damages that are accompanied by intensive wave generation.

Any addition of new rods, straight or curved, increases the resistance. Additional curved rods may either join the neighboring nodes, as in chains with waiting links, or they may join any two nodes in the structure. The problem of optimal position of additional rods is open.

#### 1.4 Dynamics of bistable lattices

Strong elastic waves and waves of damage propagate throughout the bistable structures, reflecting from its boundaries and interfering with each other. This process leads to a high concentration of stresses that destroys the construction. On the other hand, the elastic waves can be redirected, thereby sending energy away from the zone of contact as it is discussed for the case of lattice shown below in Fig. 10 in Section 3. Initiation and redirection of waves can be effectively done by bistable

structures. Because of their local instabilities, the structures are able to absorb the kinetic energy of an impact by exciting intensive waves which more evenly distribute the *partial damage* and relax the stress by allowing for large local deformations of the elements. Stressed bistable cellular lattices naturally excite and transmit waves of damage, acting as a domino train.

Waves in locally unstable systems are controllable. The possibility to redirect the transition wave in elongated strip-like structures is demonstrated in [5]. Depending on structural parameters, the damage may either start at the impacted end and propagate toward the opposite end where the structure is fasten, or it may start at the fastened end and propagate toward the end where the force is applied, or two transition waves may be initiated at both ends simultaneously [4]. The process is controlled by parameters of the structure; optimally designed structures generate waves along the protective plate orthogonal to the direction of the impact.

An optimized structure should trigger stress waves propagation and thereby spread the stress more evenly; it must also contain multiple absorbers. This can be achieved by the use of a composite with a special structure made of a strong frame, and an absorbing filler material. The optimization strategy requires a proper choice of design parameters. They are: the shape of the whole protective construction, location of beams or frames and waiting links, and the choice of materials.

### 1.5 Analytic solutions for dynamics of bistable chains and lattices

Analytic solution of the problem of dynamics of bistable chains and lattices was derived based on ideas developed in [5, 6] for modeling of propagation of the cracks. Bistable-bond chain model was analyzed in [4, 7, 8, 9, 10, 11, 12, 13, 14, 15, 16]. In a bistable chain, the transition wave is accompanied by a significant dissipation due to the excitation of structure-associated high-frequency waves. The analytical derivation of the solution is presented in detail in [9, 15]. The work [15] also deals with a more complicated case of non-parallel branches of the two-branched strain-stress constitutive relation. In this case, the Wiener-Hopf technique is exploited to derive the solution. Analytically calculated speed of the transition wave [15] for a cellular structure with bonds characterized by a bistable constitutive model, was compared with numerically computed speed estimates. This comparison is shown in Figure 4(b). A more complex problem of breakable two-dimensional structure with waiting links was numerically investigated in [17, 18]. Bistable chain from elastic-plastic material was studied in [3]. Analytical solution of the problem of propagation of plane and crack-like transition waves in two-dimensional lattices was developed in [2].

Partial failure of a cellular structure propagates as a cascade of phase transitions. The dynamics of discrete mass-spring system with "phase transition" of damage is modeled by a system with radial forces:

$$m_k \ddot{u}_k = \sum_{j \in ]_k} F_{kj}(\|u_k - u_j\|) e_{kj}, \quad e_{kj} = \frac{u_k - u_j}{\|u_k - u_j\|} \quad (1)$$

Breakage is modeled by assumption that springs instantly change their stiffness and equilibrium lengths when the elongations reach given thresholds,

$$F_{kj}(z) = \begin{cases} C_{kj}(z - z_{eq}) & \text{if sacrificial link is unbroken} \\ C'_{kj}(z - z_{eq} - z_{slack}) & \text{if sacrificial link is broken} \end{cases} \quad (2)$$

Here, we assume that waiting links are not broken. The solution can be found if in addition a certain character of transition is assumed, such as periodicity (in reversible transition), a constant speed

of the transition wave, or a randomness. Formally, we may replace  $F_{kj}(z)$  by a time-dependent function

$$\tilde{F}_{kj}(z, t, t_{kj}^{trans}) = \begin{cases} C_{kj}(z - z_{eq}) & \text{if } t \leq t_{kj}^{trans} \\ C'_{kj}(z - z_{eq} - z_{slack}) & \text{if } t > t_{kj}^{trans} \end{cases} \quad (3)$$

where  $t_{kj}^{trans}$  is the time of transition that depends on assumed transitional parameters such as the wave's speed. We assign these parameters, and run the simulations adjusting them to the transition conditions

$$t_{kj}^{trans} : \|u_k(t_{kj}^{trans}) - u_j(t_{kj}^{trans})\| = z_{threshold} \quad (4)$$

For example, the dynamics of a mass-spring chain with damageable links is modeled [16] under assumption that springs instantly change their equilibrium lengths when the elongations reach given thresholds. Between these instances, the springs are linear and a motion of masses is described by a system of linear differential equations. Because of similarity in motion of all masses,

$$u_k(t) = u_{k-1}(t - \tau) + \eta \quad \forall k,$$

where  $\eta$  is an equilibrium distance, it is enough to consider position  $u$  of mass  $m_0$  in the period  $t \in (0, \tau)$ :

$$m_0 \ddot{u}(t) = C [u(t + \tau) - 2u(t) + u(t - \tau)] - L \left[ H(t) - H\left(t - \frac{\tau}{2}\right) \right]. \quad (5)$$

where  $C$  is stiffness and  $L$  is the relaxation parameter. This system can be solved by Fourier transform. To close the system, it remains to solve turn-on turn off condition to determine the wave's speed

$$\tau_i : \|u_1(\tau_i) - u_0(\tau_i)\| = z_{threshold} \quad (6)$$

In [15], the problem is analyzed and the speed of the transitional wave is computed. It depends on the load applied at an infinitely distant point, see Figure 4(b). The calculation was verified by simulation of the transitional wave in a spring-mass system and measuring its speed, see Figure 4(a). The points obtained by numerical simulation are marked at the analytically calculated speed curve in Figure 4(b).

## 2 Model of an impact resistive bistable structure

Transmission and redirection of stress waves can be achieved and optimized through use of the bistable design. The local instabilities excite intensive waves that evenly distribute the "partial damage" to allow large local deformations without fully damaging the global protective system (see Fig. 5).

### 2.1 One dimensional constitutive material model

The constitutive relation for a one-dimensional elastic-brittle breakable specimen is modeled as

$$\sigma = (1 - c)D\varepsilon, \quad \varepsilon = \ln\left(\frac{\Delta L}{L}\right) \quad (7)$$

where  $D$  is the material modulus,  $c$  is a damage parameter that takes the value of zero (undamaged specimen) or one (damaged specimen),  $L$  is the undeformed length, and  $\Delta L$  is the elongation.

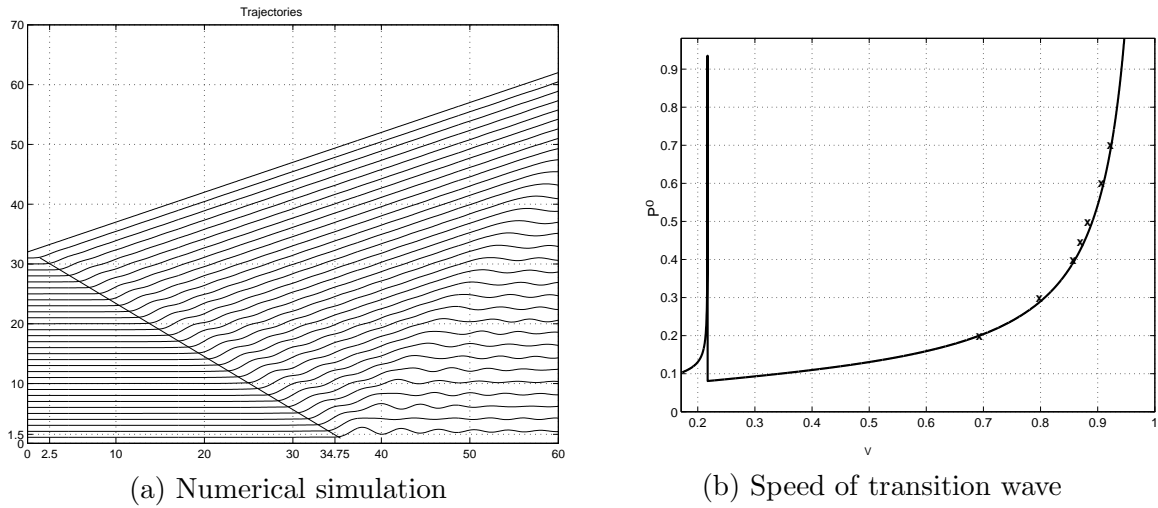


Figure 4: (a) Numerically simulated wave of transition in a 32-cell chain. (b) Analytically calculated speed of the transition wave compared with numerical estimates shown by stars.

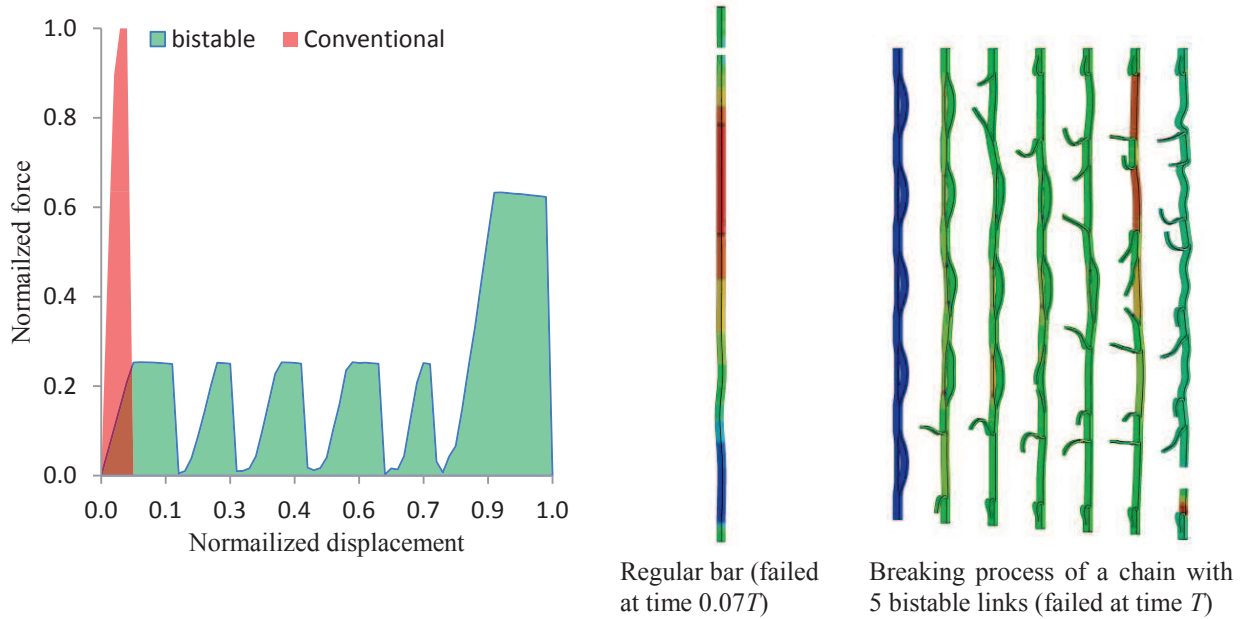


Figure 5: Finite element simulations of a bistable versus a conventional chain having identical mass and subjected to the same loading (displacement control). The simulation used basic elastic-plastic material model. The area under the curve represents the amount of energy absorbed by the structure. This particular example shows that the bistable chain absorbed approximately 4.5 times the amount of energy the conventional chain absorbed before failure.



For numerical simulation, we use the discretized model. The axial stress at time step  $n + 1$  is computed through stress  $\sigma^n$  at the previous time step  $n$ .

$$\sigma^{n+1} = \sigma^n + D [(1 - c^{n+1})\varepsilon^{n+1} - (1 - c^n)\varepsilon^n], \quad (8)$$

where  $c^n$  control the status of the links at time step  $n$ ; if  $c^n = 0$ , the link is undamaged, if  $c^n = 1$ , it is broken, and  $0 < c^n < 1$  corresponds to a partially damaged link. Evolution of  $c^n$  is described by the equation

$$c^{n+1} = \begin{cases} 0 & \text{if } \varepsilon_{\text{total}} \leq \varepsilon_c \text{ and } c^n \neq 1 \\ c^n + \dot{c}\Delta t & \text{if } \varepsilon_{\text{total}} \geq \varepsilon_c \text{ and } c^n < 1 \\ 1 & \text{otherwise,} \end{cases} \quad (9)$$

where  $\varepsilon_c$  is the critical strain and  $\dot{c}$  is the speed of damage.

In a bistable assembly, the stress is expressed as a sum of the stresses in the sacrificial and waiting elements,

$$\sigma^{n+1} = \sigma_s^{n+1} + \sigma_w^{n+1}, \quad (10)$$

where subscripts  $s$  and  $w$  denote the sacrificial and waiting links, respectively. To obtain the the bistable response shown in Fig. 2, the stress in the sacrificial element is evaluated using Eq. (8). The waiting element is initially inactive and is activated after the strain in the bistable assembly reaches a predefined value,  $\varepsilon_{\text{init}}$ . The stress in the waiting element is computed using

$$\sigma^{n+1} = [\sigma^n + D ((1 - c^{n+1})\varepsilon^{n+1} - (1 - c^n)\varepsilon^n)] \times b(\varepsilon_{\text{init}}). \quad (11)$$

where

$$b(\varepsilon_{\text{init}})^{n+1} = \begin{cases} 0 & \text{if } \varepsilon_w \leq \varepsilon_{\text{init}} \text{ and } b(\varepsilon_{\text{init}})^n \neq 1 \\ 1 & \text{otherwise,} \end{cases} \quad (12)$$

Before failure of the sacrificial element, damage parameter  $c_s$  is zero, therefore  $\sigma_w = 0$  and  $\sigma_s > 0$ . When the sacrificial element fails,  $\sigma_s$  becomes zero (see Eq. (8)) and the waiting element picks up the load (see Eq. (11))  $\sigma_w > 0$ . When the deformation reaches a critical value  $\varepsilon_c$ , waiting element fails as well. This material model is used in the finite element simulations below. The damage speed  $\dot{c}$  plays an important role, the effectiveness of the bistable assembly depends on this value relative to the speed of the impact.

### 3 Numerical examples

The numerical simulations are carried out using LS-Dyna [19] with the custom material model presented above. The structure is assembled using truss elements.

#### 3.1 Example 1: A rigid ball impacting a net

Using the model in Eqs. 7 to 12, we have performed 3-D simulations of a rigid body impacting two-dimensional lattices, one assembled from conventional links and another one assembled from

Table 1: Sacrificial element's parameters

Parameter	Value
Young modulus, $E_s$	120 GPa
Poisson's ratio, $\nu_{12s}$	0.36
Length, $L_s$	1.0 m
Cross-sectional area, $A_s$	0.01 m <sup>2</sup>
Critical strain, $\varepsilon_{cs}$	0.008

Table 2: Waiting element's parameters

Parameter	Value
Young modulus, $E_w$	120 GPa
Poisson's ratio, $\nu_{12w}$	0.36
Length, $L_w$	1.008 m
Cross-sectional area, $A_w$	0.0198 m <sup>2</sup>
Critical strain, $\varepsilon_{cw}$ (after fully stretched)	0.008

bistable links. These two lattice systems were given identical areal densities. Under various loading conditions, the exit velocity, the kinetic energy of the impacting ball, and distribution of damage and stress in the conventional and bistable nets are compared. It is assumed that the ball impacts the lattice perpendicularly. The model parameters are given in Table 1 and 2 for the simulation time of  $t = 0.5$  s. The parameters are chosen so that the transition to the waiting element is sufficiently fast to simulate the response in Fig. 2.

A 100mx100m net was constructed and constrained in all direction along the edges. The net is constructed using 23539 truss elements, and contains 8404 nodes. Here we use the general three-dimensional segment-based penalty contact algorithm [19] with the lattice containing the slave nodes and the ball containing master nodes. No contact friction is accounted for. The results are compared with a similar net from conventional links of the same mass as the sacrificial and waiting elements together; they are made from the same material.

The comparison of the impact resistance is illustrated in Fig. 6. Moreover, as the rigid body penetrates the lattice, cracks are formed in the absence of bistable links, but are avoided when using bistable links. Based on this observation, further investigation will help us to understand the mechanism of damage waves as well as to develop a technique that allows to control these waves in multilevel lattice structures. For example, the path of the damage propagation, or branching of the damage zone in a desired direction, can be controlled through introduction of weak zones or by optimizing the orientation or density of the bistable links. Thus, it is possible to design a "topological trap" for the arrest of the damage propagation.

The results demonstrated in Fig. 6 are based on the constitutive model described in Eqs. 7 to 12, which crudely accounts for damage and eliminates the need of sacrificial element deletion. The model does not have the capability to replace or rearrange the elements when the structure is subjected to different loading conditions during its life cycle. However, the presented results already demonstrate the potential of the bistable link concept.

**Effectiveness** To evaluate the effectiveness, the effective value  $R$  is the ratio of the initial impact velocity,  $v(t_0)$ , to the exit velocity,  $v(t_{\text{final}})$  [17]:

$$R = \frac{v(t_{\text{final}})}{v(t_0)}, \quad (13)$$

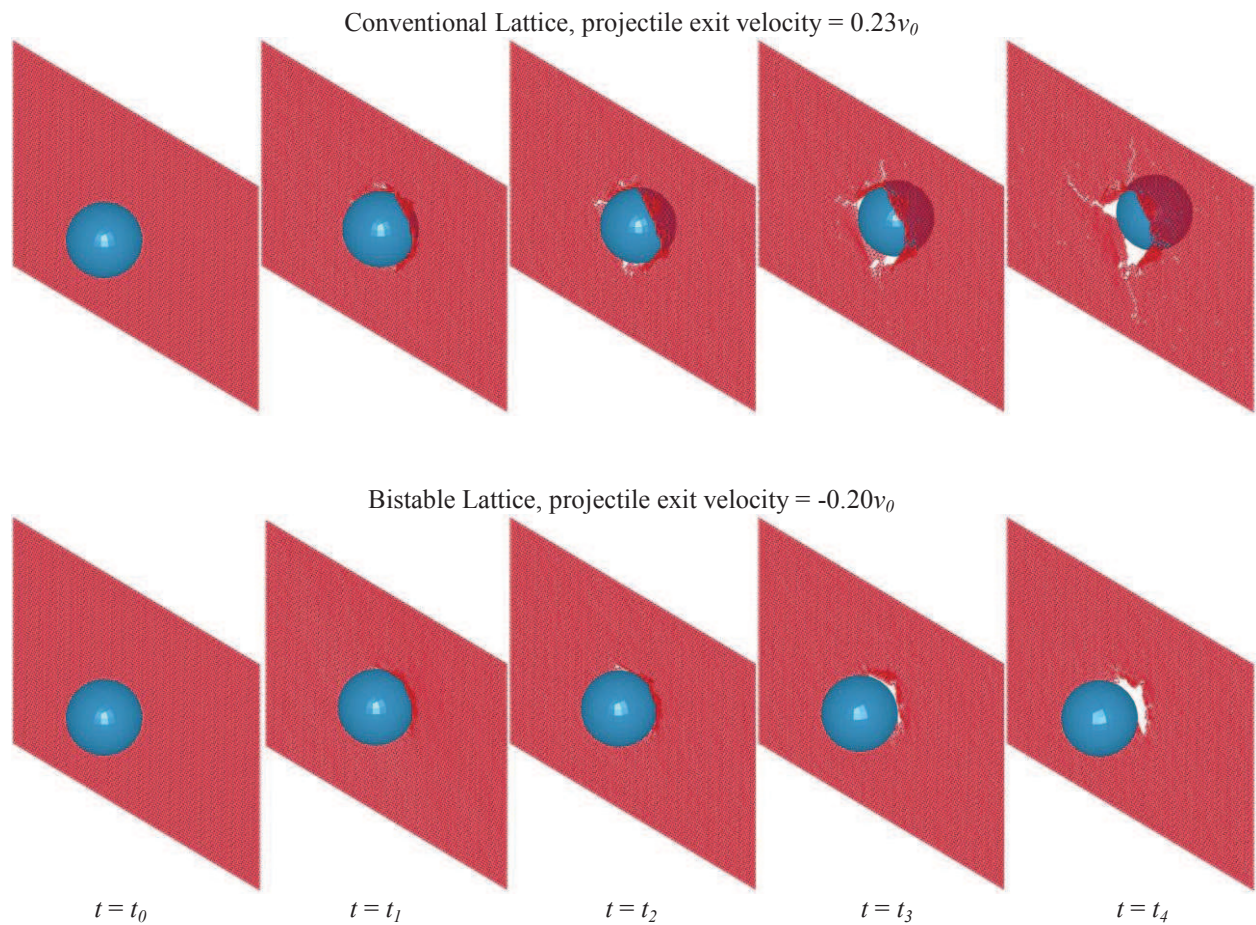


Figure 6: Finite element simulations of lattices impacted by a rigid body. The conventional (top) and the bistable (bottom) lattices have the same total mass, are made of the same material, and are subjected to the same boundary conditions and impact loading. The simulations show that, under the same conditions, the bistable lattice captures and rejects the impacting ball, while the conventional lattice fails to resist the impact.

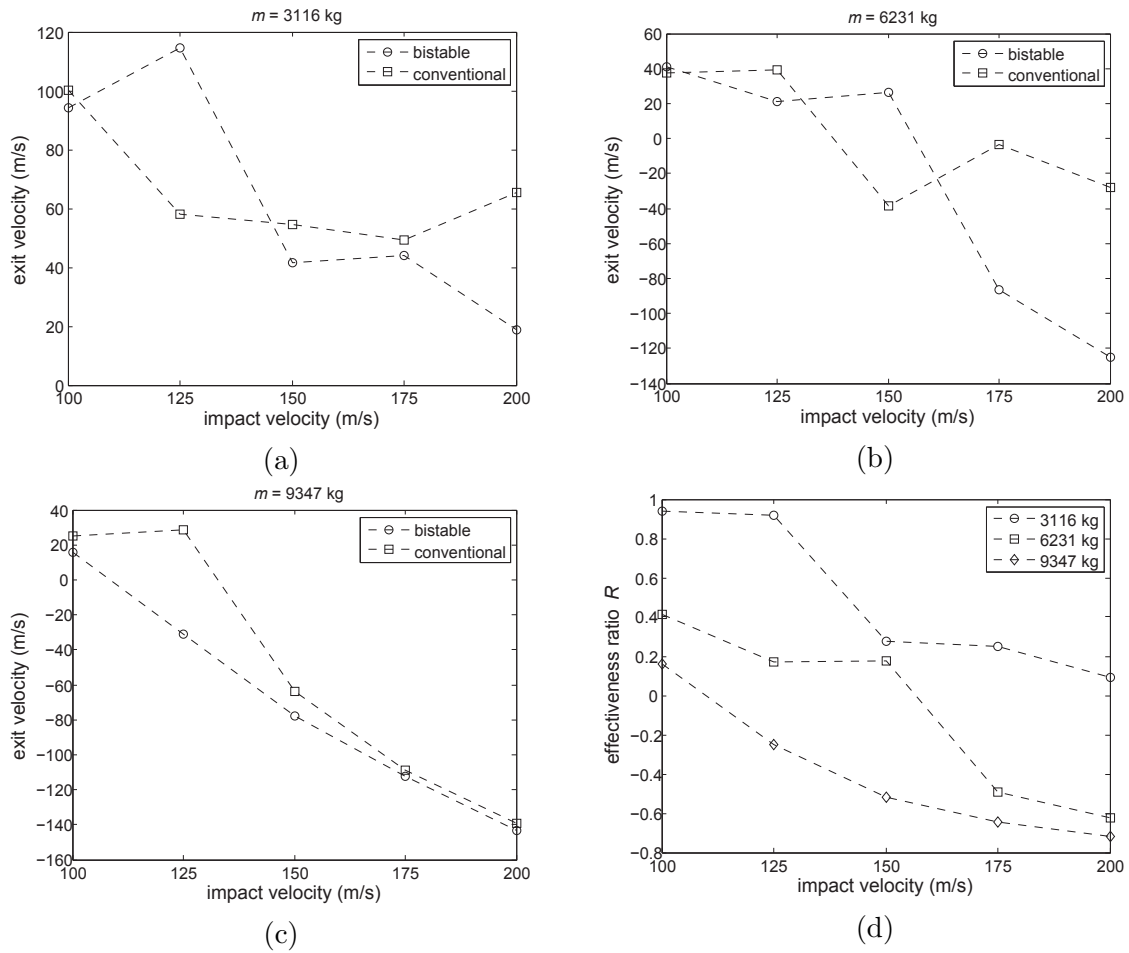


Figure 7: (a)-(c) Comparison of the ball velocity at  $t = 0.5$  s. The positive velocity implies that the ball bounces off the net, while the negative velocity indicates that the ball continues to penetrate the net. (d) Effectiveness ratio of the bistable net under an impact of various masses. The net is most effective against impact when the  $m \leq 6231$  kg and  $v_{\text{impact}} \leq 150$  m/s.

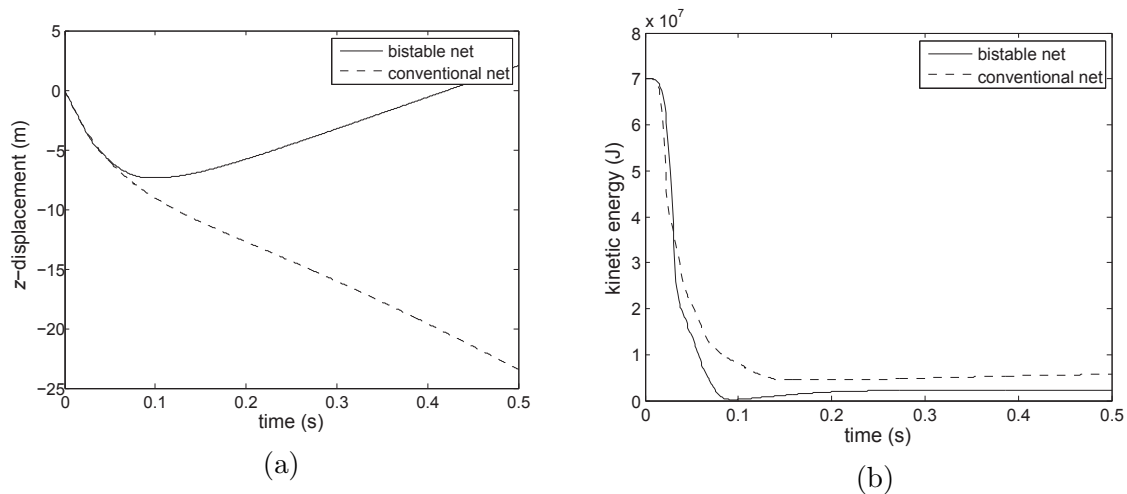


Figure 8: (a) Kinetic energy. Mass = 6231 kg and impact velocity = 150 m/s. (b) Displacement along the  $z$ -direction; mass = 6231 kg and impact velocity = 150 m/s.

where  $t_0$  and  $t_{\text{final}}$  are the initial and the final moments of the observation, respectively. The variation of impulse of the ball  $R$  shows how much of it is transformed to the motion of structural elements. Parameter  $R$  evaluates the structure's performance using the impacting ball as a measuring device without considering the energy dissipated in each element of the structure; it does not vary when the ball is not in contact with the structure.

For the chosen configuration, at lower mass (3116 kg), the ball is rejected and neither conventional nor bistable design is damaged. When the speed of the impact is moderate (see Fig. 7), the bistable structure is more effective. It stops heavier balls or decreases the speed of penetrating ones. The bistable net has the most advantage over the conventional net when the initial velocity of the ball is 150 m/s and the mass of the ball is 6231 kg. At this combination, the ball is bounced off the bistable net, while the conventional net is penetrated, see Fig. 7d. In addition, Fig. 8 shows that more energy is dissipated by the bistable net than the conventional net. However, at high speed both structures behave similarly. For example, when the ball's mass is 9347 kg and its speed is above 175 m/s, the ball penetrates both nets and have similar exit velocity.

**Damage distribution** We observe that a conventional net is destroyed sooner than the one with waiting elements, and it requires less energy to be penetrated. The larger energy dissipation is achieved by delocalization of damage. The damage in the conventional net (see Fig. 9) concentrates in the impact area. The damage in the bistable net occurs by the failure of sacrificial elements and it is more distributed (see Fig. 10). Notice that some sacrificial elements located far away from the impact zone are destroyed while others are not. The damaged links are clustered in small regions scattered throughout the net.

The dynamics of the damage and failure of the net can be viewed as a series of phase transitions. After each break, the network changes its elastic properties and its equilibrium position. In contrast with the conventional structure, the bistable structure may become stronger after sacrificial

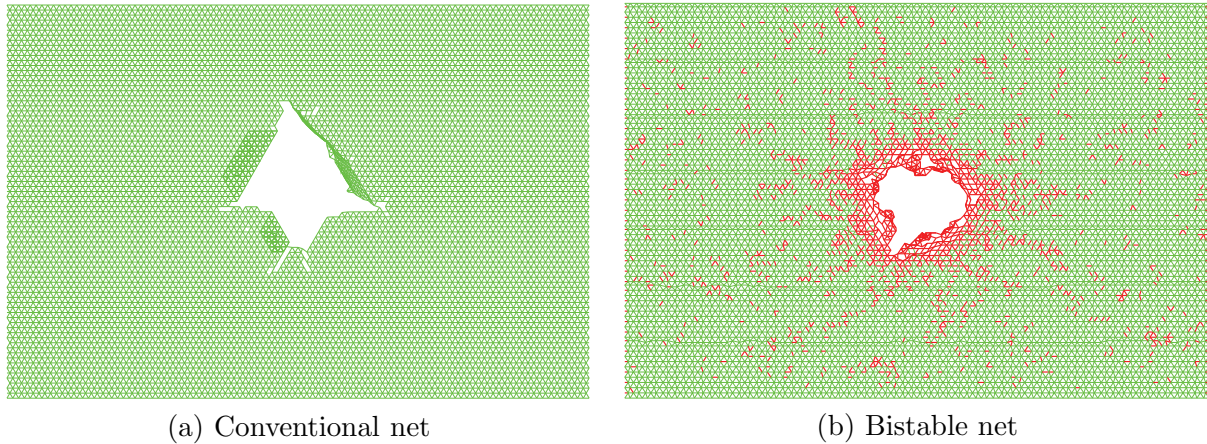


Figure 9: Damage at  $t = 0.5$  s.: (a) The completely destroyed sacrificial elements are shown in red (2435 damaged links), while the completely damaged waiting element are hidden from view. There are no partially damaged links in this example because the damage speed  $\dot{c}$  is set to the same value as the time step size used in the simulation. (b) The completely destroyed links (284 links) are hidden from view.

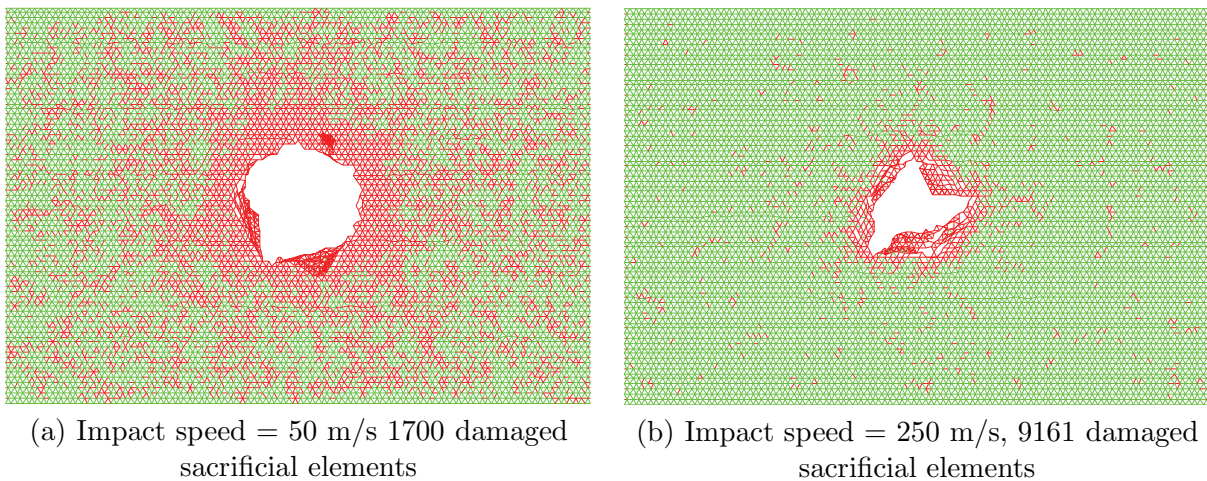


Figure 10: Damage at  $t = 1.0$  s.: (a) These figures illustrate the effect of the waiting elements when the net is subjected to slower and faster impacts having initial kinetic energy of  $70 \times 10^6$  N·m (similar to the case shown in Fig. 9. The number of the partially damaged links increases as the speed of the projectile decreases.

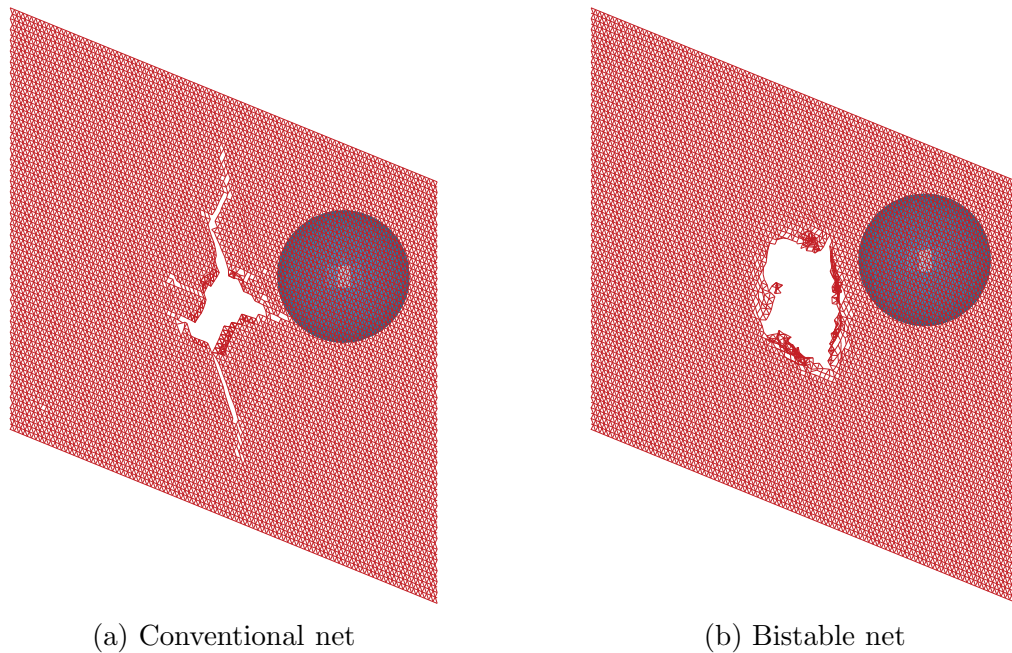


Figure 11: Penetration of a 9347 kg rigid ball with initial velocity of 175 m/s,  $t = 0.3s$ . The phase transition leads to a *pseudo-plastic* response of the net.

elements break. After a sacrificial element breaks, the slackness of the waiting element causes the elastic wave to travel away which helps to spread the damage across the structure.

As the ball penetrates through the net, cracks are formed in the conventional net (see Fig. 11), while no crack formation is observed in the bistable net. Crack is stopped in the bistable net because bistability leads to stress delocalization. Notice that bistable nets, made from an elastic-brittle material, show large but stable *pseudo-plastic* strains and thus increase the resistivity.

## 4 Damage tracking and optimization of bistable structures

The resistance against fracture and yielding of a protective lattice of bistable links can be optimized by material redistributing, i.e., reinforcing the overloaded links at the expense of underloaded ones. An optimization algorithm can be formulated similar to the approach such as those in [20, 21]. The main challenge of the optimization problem is the time dependent loading and structural variation due to damage, which leads to high sensitivity of the design variables as illustrated in the simulations of the rigid body impacting a bistable lattice discussed earlier (Fig. 10). These figures show that the effectiveness of the design (number of fully damaged sacrificial links) at a given geometry depends greatly on the speed of the impact.

In a chain, the number of partially damaged links is related to the absorbed energy. The load carrying capacity of the chain is lost as soon as one link in the chain is broken. On the contrary, the triangular lattice can still resist concentrated loads even if some of the links are completely broken. We use two basic criteria to compare the state of the structure before and after the collision: (1) The percentage of partially damaged links, and (2) The percentage of destroyed links. The first

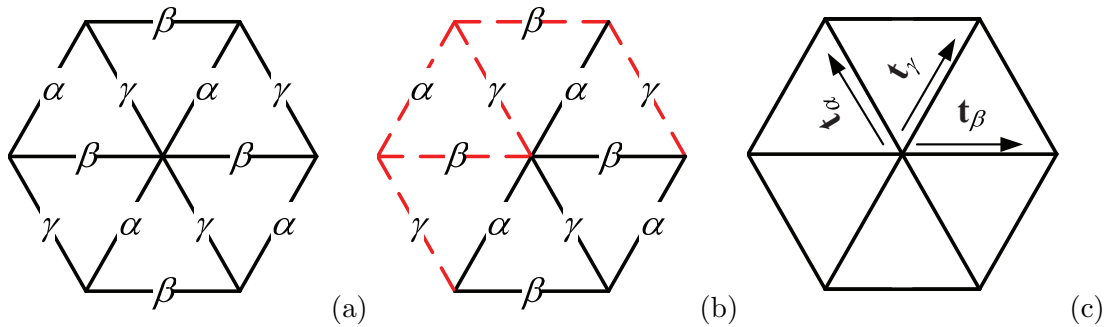


Figure 12: (a) The lattice consists of three families of parallel links  $\alpha$ ,  $\beta$ , and  $\gamma$ ; (b) Example of lattice with damaged links (dashed lines); and (c) Tangent vectors to the links' families.

number shows how effectively the partial damage is spread, and the second one shows how badly the structure is damaged. Ideally, we wish to have a structure in which all links are partially damaged, but none is completely destroyed. The number of destroyed links is a rough overall quality criterion, but it ignores a significant factor - the distribution and orientation of the broken links. To describe various configurations of broken links, we introduce a “damage tensor” that can distinguish partial damage and quantify damage texture based on which links are broken [22, 23]. For example, consider an equilateral triangular lattice that consists of three families of parallel links  $\alpha$ ,  $\beta$ , and  $\gamma$  with tangent vectors  $\mathbf{t}_\alpha$ ,  $\mathbf{t}_\beta$ ,  $\mathbf{t}_\gamma$ , respectively (see Fig. 12). In this case, we can construct the damage tensor  $\mathbf{D}$  as follows:

1. In a reference configuration, select a domain  $\Omega$  that is larger than distance between nodes (i.e., a domain containing many nodes),
2. Count the number of links  $l_\alpha, l_\beta$  and  $l_\gamma$  that contain at least one node in  $\Omega$
3. Count the number of broken links,  $b_\alpha, b_\beta$  and  $b_\gamma$  in (Fig. 12b) and introduce the relative directional damage,  $p_\alpha, p_\beta$  and  $p_\gamma$

$$p_\alpha = \frac{b_\alpha}{l_\alpha}, \quad p_\beta = \frac{b_\beta}{l_\beta}, \quad p_\gamma = \frac{b_\gamma}{l_\gamma}. \quad (14)$$

4. Finally, the damage tensor  $\mathbf{D}(\Omega)$  can be formulated using

$$\mathbf{D}(\Omega) = p_\alpha \mathbf{t}_\alpha \otimes \mathbf{t}_\alpha + p_\beta \mathbf{t}_\beta \otimes \mathbf{t}_\beta + p_\gamma \mathbf{t}_\gamma \otimes \mathbf{t}_\gamma. \quad (15)$$

Likewise, damage tensors can be constructed for the sacrificial and the waiting elements. The dimensionless damage tensor  $\mathbf{D}(\Omega)$  allows the characterization of an average damage in a region  $\Omega$  and hence the average irreversible deformation in that region. It can be used for an intermediate scale description of the damage, which in turn would be useful in optimization of link morphology as well as visualization using any standard methods for displaying tensor fields [24].

## 5 Acknowledgment

Support of this work by the United States Army Research Office (ARO) is gratefully acknowledged.



## References

- [1] Cherkaev A and Slepyan L 1995. *Int. J. of Damage Mech*, **4**(1), pp 58–82.
- [2] Slepyan L and Ayzenberg-Stepanenکو M 2004. *J. Mech. Phys. Solids*, **52**(7), pp 1447–1479.
- [3] Vinogradov V *et al* 2006. *Mech. of Materials*, **38**, pp 748–756.
- [4] Cherkaev A *et al* 2005. *J. Mech. Phys. Solids*, **53**, pp 383–405.
- [5] Slepyan L and Troyankina L 1984. *J. Appl. Mech. Techn. Phys.*, **25**(6), pp 921–927.
- [6] Slepyan, L., and Troyankina, L., 1988. In: ‘*Strength and Visco-plasticity*’, *Nauka*, pp 301–305. in Russian.
- [7] Slepyan L 2000. *J. Mech. Phys. Solids*, **48**, pp 931–964.
- [8] Slepyan L 2001. *J. Mech. Phys. Solids*, **49**, pp 513–550.
- [9] Slepyan L 2002. *Models and Phenomena in Fracture Mechanics*. Springer. Berlin.
- [10] Ngan S-C and Truskinovsky L 1999. *J. Mech. Phys. Solids*, **47**, pp 141–172.
- [11] Puglisi G and Truskinovsky L 2000. *J. Mech. Phys. Solids*, **48**, pp 1–27.
- [12] Balk A *et al* 2001. *J. Mech. Phys. Solids*, **49**, pp 131–148.
- [13] Balk A *et al* 2001. *J. Mech. Phys. Solids*, **49**, pp 149–171.
- [14] Charlotte M and Truskinovsky L 2002. *J. Mech. Phys. Solids*, **50**, pp 217–251.
- [15] Slepyan L *et al* 2005. *J. Mech. Phys. Solids*, **53**, pp 407–436.
- [16] Cherkaev A *et al* 2006. *Vibration Problems ICOVP 2005, Springer Proc in Phys* , **111** pp 111–122.
- [17] Cherkaev A and Zhornitskaya L 2004. *Asymptotics, Singularities and Homogenisation in Problems of Mechanics*, pp 273–284.
- [18] Cherkaev A and Zhornitskaya L 2004. *Multibody System Dyn*, **13**(1), pp 63 – 67.
- [19] Hallquist J O 2006. *LS-DYNA Theory Manual*. Livermore Software Techn. Corp.
- [20] Bense, M. P., and Sigmund, O., 2004. *Topology Optimization*. Springer, New York.
- [21] Cherkaev E and Cherkaev A 2008. *Computers and Structures*, **86**, pp 1426–1435.
- [22] Betten J 1983. *J. Mec. Theor. et Appl.*, **2**(1), pp 13–32.
- [23] Skrzypek J and Ganczarski A 2010. Springer, New York.
- [24] Wilson A T and Brannon R M 2005. *Proceeding of IEEE Visualization 2005*, pp 11–18